

# EUROPHYSICS LETTERS

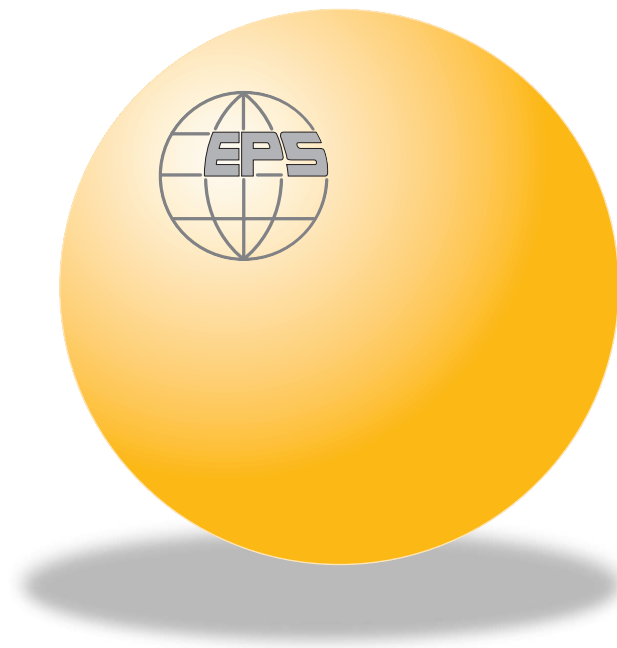
OFFPRINT

Vol. 71 • Number 4 • pp. 611–617

## Pressure-temperature-time-transition diagram in a strong metallic supercooled liquid

\* \* \*

W. H. WANG, W. UTSUMI and X.-L. WANG



Published under the scientific responsibility of the  
**EUROPEAN PHYSICAL SOCIETY**  
Incorporating  
JOURNAL DE PHYSIQUE LETTRES • LETTERE AL NUOVO CIMENTO



## Pressure-temperature-time-transition diagram in a strong metallic supercooled liquid

W. H. WANG<sup>1</sup>(\*), W. UTSUMI<sup>2</sup> and X.-L. WANG<sup>3</sup>

<sup>1</sup> *Institute of Physics, Chinese Academy of Sciences - Beijing 100080, PRC*

<sup>2</sup> *Japan Atomic Energy Research Institute, SPring-8 - Hyogo 679-5198, Japan*

<sup>3</sup> *Spallation Neutron Source and Metals Ceramics Division  
Oak Ridge National Laboratory - Oak Ridge, TN 37830, USA*

received 10 February 2005; accepted in final form 20 June 2005

published online 22 July 2005

PACS. 61.43.Fs – Glasses.

PACS. 62.50.+p – High-pressure and shock wave effects in solids and liquids.

PACS. 64.70.Dv – Solid-liquid transitions.

**Abstract.** – The crystallization kinetics and nucleation mechanism of a bulk metallic glass-forming alloy  $\text{Zr}_{46.75}\text{Ti}_{8.25}\text{Cu}_{7.5}\text{Ni}_{10}\text{Be}_{27.5}$  (vit4) in the entire supercooled liquid region (SLR) is investigated using *in situ* high-pressure and high-temperature X-ray diffraction with synchrotron radiation, which allows us for the first time to simultaneously determine the crystallization kinetics and phase evolution of a metallic liquid as a function of time under high pressure. The results are summarized in a pressure-time-temperature-transformation (PTTT) diagram with two time scales. The results suggest that the dominant crystallization mechanism of the BMG is growth-controlled.

The nucleation in metallic alloys is of longstanding scientific interest and has produced many issues [1–5]. The difficulties arise from the fact that a supercooled liquid of conventional metallic materials is quite unstable because the nucleation rate in the metallic supercooled liquid is extremely high.  $\text{Zr}_{46.75}\text{Ti}_{8.25}\text{Cu}_{7.5}\text{Ni}_{10}\text{Be}_{27.5}$  (vit4) bulk metallic glasses (BMGs) can be readily quenched into a bulk amorphous solid with a critical cooling rate as low as 10 K/s [6, 7]. The alloy has a very stable supercooled liquid state without appearance of deterioration like phase separation and high thermal stability against crystallization due to a surprisingly high viscosity ( $\eta \approx 100$  Pa) at the liquidus temperature [6]. The BMGs open the possibility of performing day-long experiments in the metastable melt state far above the calorimetric glass transition temperature,  $T_g$ , and a large experimentally accessible time and temperature window are offered for investigating the nucleation and growth under various conditions in the supercooled liquid state. Therefore, the BMGs provide a new model for studying such problem of longstanding importance.

The time scale of the amorphous-to-crystalline phase transition in BMG is characterized by the temperature-time-transition (TTT) diagram, which gives the time to reach the onset of crystallization,  $t_{onset}$ . However, the TTT diagrams, which provide important information

---

(\*) E-mail: whw@aphy.iphy.ac.cn

about the glass-forming ability and the nucleation mechanism of the system [8,9], have been determined only for few metallic systems by using an electrostatic levitator [10] or by inductively heating the samples in graphite crucibles [11]. However, the time dependence of the entire crystallization process, from the onset crystallization time to the fully crystallized time over the whole supercooled liquid region (SLR), from the equilibrium liquid down to  $T_g$  of metallic alloys under high pressure, has not been established, despite intensive work.

The information of the progression of the crystallization with time can provide deep insight into the crystallization mechanism of a supercooled liquid. Because both the nucleation and growth rates of crystalline phases in the glass-forming alloys strongly depend on the kinetics which is sensible to pressure, the information of pressure effect on the crystallization is critical for gaining insight into the mechanism of the nucleation and glass formation in the BMG-forming supercooled liquid [12–15]. However, little work on *in situ* high-pressure (HP) crystallization has been conducted perhaps due to the experimental-condition restrictions. This leaves many unresolved questions in this field. In this letter, the vit4 was chosen as a representative alloy to study the isothermal transformation from supercooled liquid into crystals under high pressure, and the results are summarized in a pressure-temperature-time-transition (PTTT) diagram. The results clearly show the markedly different effects of pressure on the nucleation and growth in the supercooled liquid state.

Zr<sub>46.75</sub>Ti<sub>8.25</sub>Cu<sub>7.5</sub>Ni<sub>10</sub>Be<sub>27.5</sub> BMG was prepared by casting the molten alloy in a water-cooled Cu mould to get a rod with a diameter of 8 mm. The amorphous nature as well as the homogeneity of the rod was ascertained with XRD, and transmission electron microscopy (TEM) [12]. The isothermal crystallization of the alloy was investigated by an *in situ* XRD technique at Spring-8, a third-generation synchrotron radiation facility in Japan. The sample was heated from room temperature to the annealing temperature under high pressure at a rate of 0.167 K/s. High-pressure and high-temperature conditions were generated using a cubic-type multi-anvil press (SMAP 180) installed on BL14B1, at Spring-8 and the sample assembly was similar to that used in ref. [16]. The sample volume is about  $1 \times 1 \times 1$  mm. NiCr-NiAl thermocouple was brought into the pressurized zone and near the sample. NaCl powder was used as pressure-transmitting medium. The pressure was calibrated from the lattice constant of NaCl, the accuracy was better than  $\pm 0.2$  GPa. An energy-dispersive method was utilized using white X-ray beam with energies of 30–150 keV. The diffracted X-ray was detected by a solid-state Ge detector, at a diffraction angle  $2\theta = 5^\circ$ . In this study, two important time scales are identified: the onset transition time  $t_{onset}$ , and the time to reach 50% of the crystallized volume fraction  $t_{50\%}$ . Whereas  $t_{onset}$  shows how the “nose” in the TTT diagram changes with pressure,  $t_{50\%}$  will shed light on the effect of pressure on crystallization kinetics. We determine the crystallized volume fraction ( $t_{50\%}$ ) by assuming that each XRD pattern is a linear combination of amorphous part  $I_a$  ( $I_a$  represents the integrated intensities of the XRD pattern for full amorphous sample at  $t = 0$ ) and fully crystallized part  $I_c$  ( $I_c$  represents the integrated intensities of the fully crystallized sample calculated by fitting the diffraction peaks with Gaussian function). Therefore, from the expression  $I(t_{50\%}) = (I_a + I_c)/2$ ,  $t_{50\%}$  can be determined. Previous studies [6,12] have established that  $T_g$ , and the crystallization temperature  $T_x$  at ambient pressure are 620 and 753 K, respectively, thus giving a supercooled liquid region of  $\Delta T = T_x - T_g = 133$  K. The melting temperature  $T_m$  at ambient pressure is 1273 K. Previous studies [17] have also found that the  $T_g$ ,  $T_x$  and  $T_m$  are insensitive to pressure, at least up to  $\sim 10$  GPa.

The representative *in situ* recorded XRD patterns of the BMG isothermally annealed at 693 K (in the low-temperature regime of SLR, which is close to  $T_g$ ) under 4.6 GPa are shown in fig. 1. The supercooled liquid state is retained until iso-annealing for 1500 s at 693 K, when some very small crystalline peaks appear indicating the beginning of the crystallization. At

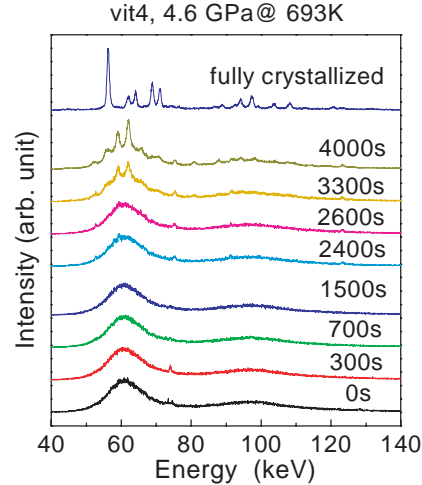


Fig. 1 – (Color online) Isothermal crystallization at 4.6 GPa for different times at 693 K.

longer annealing times, the crystalline peaks become sharper and more intense, meaning that the crystalline volume fraction grows with increasing annealing time. The sample is about 50% crystallized at 4000 s. As the isothermal annealing temperature is increased, the  $t_{onset}$  decreases. When iso-annealed at 743 K, the  $t_{onset}$  distinctly decreased to 300 s, and  $t_{50\%}$  is also reduced to about 350 s. In the high-temperature regime of SLR (near  $T_m$ ), the isothermal crystallization under 4.6 GPa is markedly different from that in the low-temperature region. At 1123 K (upon cooling from 1373 K at 7 K/s), the melt starts to crystallize after 800 s and does not reach full crystallization until 1800 s. When iso-annealed in the temperature range much below  $T_m$  (773 K to 1123 K), the onset crystallization time and entire crystallization events take place in a very short time ( $< 30$  s). This makes impossible for us to study the isothermal crystallization kinetics under high pressure in the range from 773 K to 1123 K. The above results indicate that the crystallization behaves differently in the whole SLR. In the high-temperature regime of SLR, the crystallization then occurs with a very short incubation time and an entire crystallization time. While in the low-temperature regime, the onset crystallization time increases with decreasing temperature, and the growth of crystals solely determines the time scale of crystallization. Similar results have been found in PdNiCuP BMG at ambient pressure [18]. We tried to use the JMAK equation [19] to simulate the isothermal crystallization. An exponent value of  $n = 0.30$  at 693 K and 4.6 GPa is similar to the value of 0.33 obtained in ref. [20] for ZrTiCuNiAl BMG. In classical theory of diffusion-controlled transformations,  $n$  is often used to characterize the mechanism of transformation. The small value of  $n$  further confirms the growth-controlled crystallization under HP in the low-temperature regime [21].

The isothermal crystallizations at 4.6 GPa were carried out at different temperatures and the results are summarized in the PTTT diagram in fig. 2. In the PTTT diagram,  $t_{onset}$  is plotted against temperature in the entire SLR. From the diagram one can see the sketch of the typical nose shape in the range of 180 s. Compared with the TTT diagram of the alloy (the typical nose shape is in the range of 100 s) [6] under ambient condition, HP obviously shifts the TTT curve to high elapsed time, which indicates the HP enhances the glass-forming ability of the alloy. Experimental results do indeed confirm that HP can significantly enhance the glass-forming ability of the BMG-forming alloys [17].

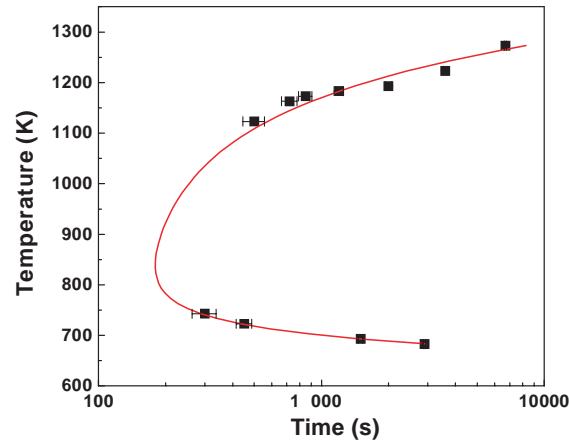


Fig. 2 – (Color online) The TTT diagram of vit4 at 4.6 GPa; the solid line is a guide for the eyes.

Meanwhile, the phase evolution is also exhibited during the HP crystallization study. The final crystallized phases were found to be  $\text{ZrBe}_2$ , Laves phase  $\text{ZrTiNi}$ ,  $\text{Zr}_2\text{Cu}$  and other unidentified phases, and the final crystallization products are almost identical to HP crystallization in the range 0–10 GPa. The phase evolution pathways are different. Unlike the crystallization at ambient pressure [22], no intermediate metastable crystalline phase precipitates during the various isothermal HP crystallization processes. The results indicate that pressure does not change the final crystallized phases, but the phase evolution process.

The  $t_{onset}$  at 4.6 GPa (■) and at ambient pressure (●) are plotted against temperature in fig. 3(a). It can be clearly seen that  $t_{onset}$  increases with decreasing isothermal temperature

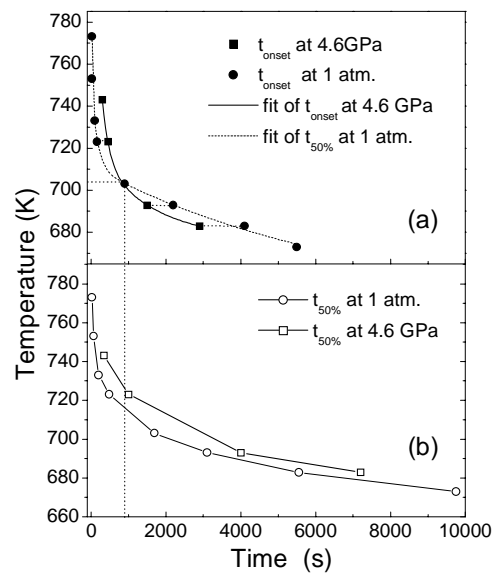


Fig. 3 – The TTT diagram of vit4 at 4.6 GPa; (a) The time to reach onset crystallization  $t_{onset}$  (■), and (b) the time to transform 50% crystallization volume fraction  $t_{50\%}$  (□) at 4.6 GPa upon temperature. For comparison,  $t_{onset}$  (●) and  $t_{50\%}$  (○) for crystallization at ambient conditions are also presented.

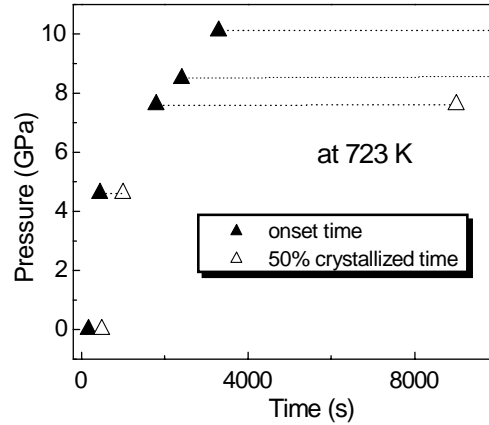


Fig. 4 – The time to reach onset crystallization (▲) and the time to transform 50% crystallization volume fraction (△) at 723 K upon pressure.

both under ambient and high pressures. However, one apparent trend is that for  $T > 703$  K, the isothermal crystallization has longer incubation time at 4.6 GPa compared with that at ambient condition; the  $t_{onset}$  at 4.6 GPa becomes significantly smaller, and the difference in  $t_{onset}$  becomes distinct at low temperature near  $T_g$ . The  $t_{50\%}$  at 4.6 GPa (□) and at ambient pressure (○) are plotted against temperature in fig. 3(b). The  $t_{50\%}$  clearly increases with decreasing isothermal temperature. The apparent difference is that the isothermal crystallization has longer growth time at 4.6 GPa compared to that at ambient condition during the whole annealing temperature range. To confirm the phenomenon, the incubation time and half-crystallized time at 723 K (near  $t_{onset}$  nose) at various pressures were determined and plotted in fig. 4. Clearly, both  $t_{onset}$  and  $t_{50\%}$  increase with increasing pressure; however,  $t_{50\%}$  is much more increased compared with  $t_{onset}$  upon pressure. For example, at 7.5 GPa,  $t_{onset} = 1800$  s, more than one order of magnitude longer than that at ambient pressure ( $t_{onset} = 170$  s), while the  $t_{50\%}$  is increased to about 9000 s and much larger than  $t_{onset} = 150$  s at ambient pressure. The results confirm that HP is more effective to suppress the growth of the crystalline phase. The increasing diffusion activation energy, at 4.6 GPa, is estimated to be about 0.23 eV. Therefore, HP further slows down the growth process in the growth-controlled crystallization through the suppression of the long-range diffusion process in the supercooled liquid state.

The comparison shows very clearly the effect of HP on nucleation and growth. The effect on nucleation varies in different temperature regimes, which is consistent with the previous report [20]. At low temperature, where the nucleation is dominated by the thermodynamic driving force rather than by diffusion, the reduction of nucleation barrier by HP becomes important. This explains why  $t_{onset}$  is smaller at low  $T$ . At high  $T$ , where the nucleation is dominated by diffusion, the effect of pressure is principally seen in the reduction of diffusion, which leads to an increased  $t_{onset}$ . The crossover is at  $T = 703$  K. The growth is slower under HP due to elimination of free volumes. The above results show that HP has different effects on nucleation and growth in the vicinity of nose, and implies that different crystallization mechanisms operate in the two regimes.

The activation energy,  $\Delta G^*$  can be estimated from the temperature-dependent annealing time,  $\tau = t_{onset} = \tau_0 \exp[E\Delta G^*/k_B T]$ , where  $\tau_0$  is constant. The effective activation energy can be considered to be mainly related to the nucleation process, because during the initial crystallization stage —incubation period— nucleation is the dominant process [20], which is followed by an abrupt amorphous-to-crystalline phase transformation characterized by slow

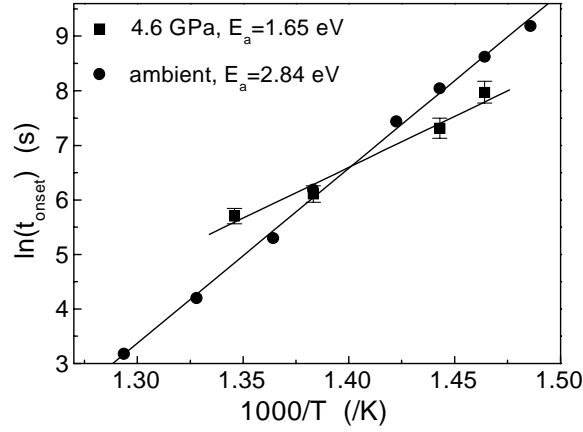


Fig. 5 – The plots of  $\ln t_{onset}$  vs.  $1/T$  at ambient and high pressure; the activation energy  $E_a$  for nucleation can be determined from the linear fit.

growth of the crystalline particles. Figure 5 shows the plots of  $\ln t_{onset}$  vs.  $1/T$  at ambient and HP. From the linear fits, we obtained a  $\Delta G^*$  of 2.84 eV at ambient conditions, and 1.65 eV under 4.6 GPa. The much reduced  $\Delta G^*$  indicates that HP lowers the nucleation activation barrier for crystallization. Within the classic nucleation theory, the steady-state nucleation rate [23],  $I \propto \exp[-\frac{\Delta G^*}{k_B T}]$ , where  $k_B$  is the Boltzmann constant. Thus the decreasing  $\Delta G^*$  means that pressure can enhance the nucleation. Other experimental and numerical modeling studies also demonstrate that HP promotes short-range atomic ordering in the metallic glasses by the reduction of the free volume and restructuring of the atomic configuration [24].

For vit4, the pressure leads to a decrease of the nucleation activation energy, and the nucleation in the supercooled liquid is promoted by pressure [17]. On the other hand, HP can significantly suppress the growth of the crystalline phases in BMG. To understand the results, we use the approach of classical nucleation serving as a simplified model. For the steady state, the crystalline growth rate can be expressed by [25]:  $U = \frac{D}{a} [1 - \exp[-\frac{\Delta G}{kT}]]$  with the interatomic spacing  $a$ ,  $\Delta G$  the free energy difference between the nuclei and liquid phase and  $D$  the diffusivity.  $(\frac{\partial(\ln D)}{\partial P})_T = -\frac{\Delta V^*}{k_B T}$ ,  $\Delta V^*$  is the activation volume. The growth velocity under high pressure,  $U_{HP} = \frac{D_0}{a} \exp[-\frac{Q+P\Delta V^*}{kT}] [1 - \exp[-\frac{\Delta G+P\Delta V}{kT}]]$ , where  $Q$  is the diffusion activation energy. From the above equations, one can see that  $D$  is the main parameter strongly affecting the growth rate. This is the reason why the growth is more sensitive to pressure. We estimated  $\Delta G$  from the DSC results in ref. [26]. For vit4,  $\sigma = 0.04$  J/m,  $A = 10$  [26],  $\Delta V^* \approx 13.0 \text{ \AA}^3$  [17], and  $\Delta V/V \approx 1\%$  [17]. The data of  $D$ ,  $Q$  ( $\sim 1.0$  eV) are obtained from refs. [27, 28]. The estimation shows that the growth rate under HP is much lower compared with that at ambient pressure in the supercooled liquid, and then the crystallization is much easier to be suppressed under HP.

In conclusion, the crystallization kinetics and nucleation mechanism of bulk metallic glass-forming alloy  $\text{Zr}_{46.75}\text{Ti}_{8.25}\text{Cu}_{7.5}\text{Ni}_{10}\text{Be}_{27.5}$  in the entire supercooled liquid regime is investigated using *in situ* high-pressure and high-temperature XRD with synchrotron radiation, which allows us for the first time to simultaneously determine the crystallization kinetics and phase evolution of a metallic liquid as a function of time from the liquidus temperature to the glass transition temperature under high pressure. The PTTT diagram with two time scales is obtained. One is given by the time to reach onset crystallization and reflects the typical “nose” shape of the PTTT diagram. The other is the half-width of the crystallization event itself

(50% of crystallized volume fraction) which can reflect the information for growth of crystals and the effect of pressure on the crystallization. The phase evolution of the crystallization with time is *in situ* exhibited in the entire SLR under isothermal conditions at high pressure. The results suggest that the dominant crystallization mechanism at low-temperature scale of SLR of the BMG is growth-controlled.

\* \* \*

The authors are grateful for the financial support of the National Natural Science Foundation of China (Grant nr. 50321101). XLW acknowledges support by the US Department of Energy (DE-AC05-00OR22725). The experimental assistance and help of T. OKADA, D. Q. ZHAO and Z. X. WANG are appreciated. Dr. Y. KATAYAMA, Dr. H. KANEKO, Dr. M. X. PAN and Prof. N. HAMAYA are appreciated for valuable discussions.

#### REFERENCES

- [1] KELTON K. F., *Phys. Rev. Lett.*, **90** (2003) 195504.
- [2] EGAMI T., *Z. Metallkd.*, **93** (2002) 1071.
- [3] DOHERTY R. D., in *Physical Metallurgy*, edited by CAHN R. W. and HAASEN P. (Elsevier Science B.V. North-Holland, Amsterdam) 1996, p. 1364.
- [4] PEREPEZKO J. H. and SMITH J. S., *J. Non-Cryst. Solids*, **44** (1981) 65.
- [5] KOESTER U. and MEINHARDT J., *Mater. Sci. Eng. A*, **178** (1994) 271.
- [6] JOHNSON W. L., *MRS Bull.*, **24** (1999) 42.
- [7] GREER A. L., *Science*, **267** (1995) 1947.
- [8] TURNBULL D., *J. Appl. Phys.*, **21** (1950) 1022.
- [9] UHLMANN D. R., *J. Non-Cryst. Solids*, **7** (1972) 337.
- [10] KIM Y. J., BUSCH R. and JOHNSON W. L., *Appl. Phys. Lett.*, **68** (1996) 1057.
- [11] SCHROERS J., JOHNSON W. L. and BUSCH R., *Appl. Phys. Lett.*, **77** (2000) 1158.
- [12] WANG W. H., DONG C. and SHEK C. H., *Mater. Sci. Eng. R*, **44** (2004) 45.
- [13] ZHANG J. and ZHAO Y., *Nature*, **430** (2004) 332.
- [14] KIM J. J., CHOI Y., SURESH S. and ARGON A. S., *Science*, **295** (2002) 654.
- [15] RUITENBERG G., HEY P. D., SOMMER F. and SIETSMA J., *Phys. Rev. Lett.*, **79** (1997) 4830.
- [16] UTSUMI W. and SHIMOMURA O., *Rev. High Pressure Sci. Technol.*, **7** (1998) 1484.
- [17] WANG W. H., OKADA T., WEN P., WANG X. L., PAN M. X., ZHAO D. Q. and UTSUMI W., *Phys. Rev. B*, **68** (2003) 184105.
- [18] SCHROERS J., WU Y., BUSCH R. and JOHNSON W. L., *Acta Mater.*, **49** (2001) 2773.
- [19] JOHNSON W. A. and MEHL R. F., *Trans. Am. Inst. Min. Metall. Eng.*, **135** (1939) 416.
- [20] WANG X. L., ALMER J., WANG Y. D., ZHAO J. K., LIU C. T., STOICA A. D., HAEFFNER D. R. and WANG W. H., *Phys. Rev. Lett.*, **91** (2003) 265501.
- [21] CHRISTIAN J. W., *The Theory of Transformation in Metals and Alloys*, 2nd edition (Pergamon Press, Oxford) 1975.
- [22] WANG W. H., WU E., WANG R. J. and STUDER A. J., *Phys. Rev. B*, **66** (2002) 104205.
- [23] TURNBULL D. and FISHER J. C., *J. Chem. Phys.*, **17** (1949) 71.
- [24] SHEN Z. Y., *Phys. Rev. B*, **39** (1989) 2714.
- [25] UHLMANN D. R., HEYS J. F. and TURNBULL D., *Phys. Chem. Glasses*, **7** (1966) 159.
- [26] BUSCH R., LIM Y. J. and JOHNSON W. L., *J. Appl. Phys.*, **77** (1995) 4039.
- [27] FAUPEL F., *Rev. Mod. Phys.*, **75** (2003) 237.
- [28] MSSUHR A., WANIUK T. A., BUSCH R. and JOHNSON W. L., *Phys. Rev. Lett.*, **82** (1999) 2290.